

# Influence of carbon and nitrogen on electronic structure and hyperfine interactions in fcc iron-based alloys

A N Timoshevskii †§, V A Timoshevskii ‡ and B Z Yanchitsky†

† Institute of Magnetism, 36-b Vernadskii St., 252680 Kiev, Ukraine

‡ Rostov State University of Transport, Narodnogo Opolcheniya 2, Rostov-on-Don, 344038 Russia

**Abstract.** Carbon and nitrogen austenites, modeled by  $\text{Fe}_8\text{N}$  and  $\text{Fe}_8\text{C}$  superstructures are studied by full-potential LAPW method. Structure parameters, electronic and magnetic properties as well as hyperfine interaction parameters are obtained. Calculations prove that Fe-C austenite can be successfully modeled by ordered  $\text{Fe}_8\text{C}$  superstructure. The results show that chemical Fe-C bond in  $\text{Fe}_8\text{C}$  has higher covalent part than in  $\text{Fe}_8\text{N}$ . Detailed analysis of electric field gradient formation for both systems is performed. The calculation of electric field gradient allow us to carry out a good interpretation of Mössbauer spectra for Fe-C and Fe-N systems.

PACS numbers: 71.20.Be, 76.80.+y, 71.15.Ap

## 1. Introduction

Face centered cubic (fcc) iron-based alloys are widely used for developing of stainless austenitic steels especially for using in critical temperature ranges, aggressive environment and other severe external conditions. Doping of these steels with light interstitial impurities influence mechanics and kinetics of structure phase transitions in Fe-based alloys. Nitrogen doping enables to solve the problem of the strengthening of stainless steels.

Carbon and nitrogen doping differently influence structure and mechanical properties of austenites. Studying of this effect by means of Mössbauer spectroscopy determined substantial differences in spectra of carbon and nitrogen austenitic steels (Sozinov *et al* 1997, 1999). A lot of information, containing in Mössbauer spectra as well as high accuracy of measurements lead to the fact that detailed interpretation of these experimental results appears to be a very complicated problem and needs application of high-accuracy theoretical methods.

The role of *ab initio* calculations in the area of solid state research rapidly increased last years. Step by step semiempirical methods, containing a lot of parameters, are

§ To whom correspondence should be addressed.

replaced by calculations from first principles. We observe the extension of application field of *ab initio* quantum mechanical methods of calculations of electronic structure and physical properties of solids. Last years these methods are more often used for solving not only fundamental, but also applied problems.

In this paper we study the influence of carbon and nitrogen on atomic and electronic structure of fcc-iron. Mössbauer spectroscopy gives the most interesting data about impurity distributions, electronic structure and magnetic interactions in solids. The study of shifts and splitting of nuclear energy levels gives information about symmetry of charge distributions near the nucleus, electronic configurations of atoms and ions as well as about peculiarities of atomic structure of solids. We believe that detailed interpretation of these experimental data using single up-to-date *ab-initio* approach is an important step in investigation of the influence of light impurities (C,N) in case of real Fe(fcc) - based alloys.

## 2. Atomic structure

Up to now there is no full understanding of influence of carbon and nitrogen atoms on atomic and electronic structure of fcc Fe-C and Fe-N alloys. Based on Mössbauer spectroscopy data different authors made different conclusions about atomic structure of carbon and nitrogen Fe-based fcc alloys. For example, the group of Genin concluded that carbon distribution in fcc Fe-C alloy is close to the ordered  $\text{Fe}_8\text{C}_{1-x}$  structure (Bauer *et al* 1990). On the other hand, the group of Gavriljuk using another method of Mössbauer spectrum deconvolution and after performing Monte Carlo computer simulations showed that formation of the ordered  $\text{Fe}_8\text{C}_{1-x}$  structure is improbable (Sozinov *et al* 1997).

In this paper we are trying to solve two problems: to study differences in electronic structure of carbon and nitrogen austenites, and to perform detailed interpretation of Mössbauer experimental data for Fe-N and Fe-C alloys. As an object of our investigations we chose model  $\text{Fe}_8\text{C}$  and  $\text{Fe}_8\text{N}$  fcc-type superstructures. The same type of C and N ordering in this structures allow us to determine peculiarities of electronic structure and hyperfine interaction parameters, connected only with different influence of two types of impurity atoms.

Calculations were performed by applying highly accurate WIEN97 programme package (Blaha *et al* 1999), which employs full-potential LAPW method (Singh 1994a). Generalized gradient approximation (GGA) according to Perdew-Burke-Ernzerhof (Perdew *et al* 1996) model was used for exchange-correlation potential. The value of plane-wave cutoff was  $R_{mt} \times K_{max} = 8.4$  which corresponds to about 190 plane waves per atom in the basis set. Inside atomic spheres the wave function was decomposed up to  $l_{max} = 12$ . Charge density and potential was decomposed inside atomic spheres using lattice harmonics basis up to  $L_{max} = 6$ . In the interstitial region Fourier expansion was used with 847 coefficients. Calculations were performed for 3000 K-points in the Brillouin zone. The radii of atomic spheres were chosen as 1.9 a.u. for Fe atoms and 1.6 a.u for N(C) atoms. Standard LAPW basis set was expanded

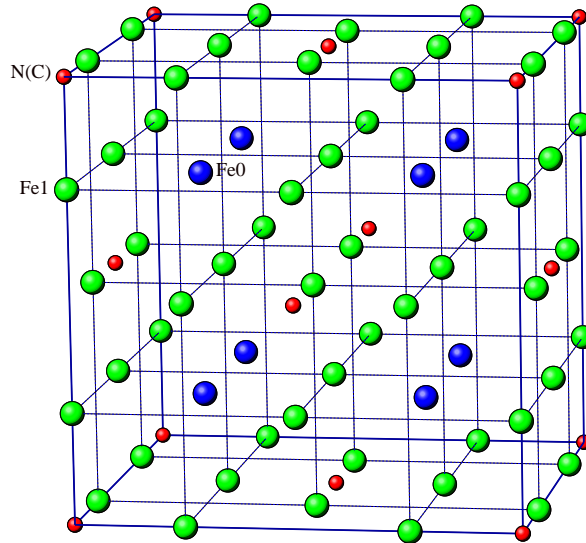


**Figure 1.** Ordered  $\text{Fe}_8\text{A}$  superstructures ( $\text{A}=\text{C},\text{N}$ ). Atoms  $\text{Fe}_1$  have one impurity atom in the first coordination sphere. Atoms  $\text{Fe}_0$  have no impurity in the nearest neighbourhood.

by including local orbitals (Singh 1994b) for  $\text{Fe}3s3p$  - states and  $\text{N}(\text{C})2s$  - states. The values of all parameters were tested for convergence and ensure accuracy of 0.1 mRy in total energy of the system. In order to check the role of local magnetic moments on Fe atoms, all calculations were performed using spin-polarized approximation.

Figure 1 presents  $\text{Fe}_8\text{A}$  supercell ( $\text{Fm}\bar{3}\text{m}$ , No.225), which was used for calculations. The structure has two symmetry types of Fe atoms:  $\text{Fe}_1$  type forms octahedron around impurity atom (has one impurity atom in the first coordination sphere);  $\text{Fe}_0$  type has no impurity atoms in the first coordination sphere. Before we performed the final electronic structure and hyperfine interaction parameters calculations, total energy minimization procedure was performed to obtain equilibrium positions of atoms. The lattice constant as well as the size of  $\text{Fe}_1$ -octahedron were varied to achieve total energy minimum. Optimization results were approximated by second-order polynomials using least square fit method. Then we analytically found the values of lattice parameters and positions of Fe-octahedron atoms. Calculated and experimental values of lattice parameters as well as calculated distance between Fe and C(N) atoms are presented in table 1. Optimization results for iron nitride  $\text{Fe}_4\text{N}$  are also presented. Good agreement with experiment shows that the method can be successfully applied for iron-nitrogen (iron-carbon) compounds.

### 3. Electronic structure

Figure 2 presents total and partial density of states for Fe, C and N atoms in  $\text{Fe}_8\text{A}$  compounds. The main difference in electronic structure of two compounds is the energy position of impurity  $2p$  states. In  $\text{Fe}_8\text{C}$  carbon  $2p$  states are located right below the  $d$ -band of iron. In  $\text{Fe}_8\text{N}$  nitrogen  $2p$  states are located 2 eV below the bottom of Fe

**Table 1.** Structure and magnetic parameters for Fe<sub>8</sub>N, Fe<sub>8</sub>C and Fe<sub>4</sub>N compounds. Fe-N(C) is the distance between Fe and impurity atom (a.u.) and  $\mu$  is local magnetic moment ( $\mu_B$ ).

	Lattice parameter	Fe-A distance	$\mu_{Fe_0}$	$\mu_{Fe_1}$	$\mu_{Fe_2}$	$\mu_{N,C}$	$\mu(\text{aver./atom})$
Fe <sub>8</sub> N (theor.)	13.946	3.54	2.78	2.09	—	-0.11	2.25
(expt)	13.849 <sup>a</sup>						
Fe <sub>8</sub> C (theor.)	13.981	3.58	2.71	2.12	—	-0.16	2.25
(expt)	13.839 <sup>a</sup>						
Fe <sub>4</sub> N (theor.)	7.164	3.582	2.90	—	2.31	0.04	2.50
(expt)	7.171 <sup>b</sup>	3.585 <sup>b</sup>	3.00 <sup>c</sup>	—	2.00 <sup>c</sup>		2.21 <sup>c</sup>

<sup>a</sup> Cheng *et al* (1990).

<sup>b</sup> Jacobs *et al* (1995).

<sup>c</sup> Frazer (1958).

*d*-band. This difference in energy positions of C and N *2p* states leads to essential difference in the character of chemical bonding in these two compounds. In Fe<sub>8</sub>C we see stronger *p* – *d* hybridization compare to Fe<sub>8</sub>N compound. The width of N *2p*-band is twice shorter than corresponding *2p*-band of carbon. This probably leads to much higher Fe-C interaction compare to Fe-N interaction.

The difference in energy distribution of valent electrons leads to considerable difference in electronic density distribution in Fe<sub>8</sub>N and Fe<sub>8</sub>C. Figure 3 presents electronic density distribution in (100) plane for two energy intervals: *2p* states of impurity atoms and *3d* states of iron in Fe<sub>8</sub>N and Fe<sub>8</sub>C compounds. Nitrogen *2p* electrons are much more localized (figure 3a) compare to *2p* electrons of carbon (figure 3c). Charge distribution around Fe<sub>1</sub> atom in Fe<sub>8</sub>C is more symmetric (figure 3d) compare to corresponding charge distribution in Fe<sub>8</sub>N (figure 3b). It should be noted that impurity atoms cause asymmetric charge distribution around Fe<sub>1</sub> atom. This also leads to asymmetric charge distribution of *d* electrons around Fe<sub>1</sub> atom. These effects greatly influence electric field gradient (EFG) at Fe<sub>1</sub> nuclei, which can be measured as quadrupole splitting in Mössbauer spectra of these two compounds.

#### 4. Hyperfine interactions in Fe<sub>8</sub>N and Fe<sub>8</sub>C

For our structures <sup>57</sup>Fe nucleus quadrupole splitting is given by the following expression:

$$\Delta = \frac{1}{2}eQV_{zz}, \quad (1)$$

where *Q* - quadrupole moment of the nucleus and *V<sub>zz</sub>* - principal component of electric field gradient (EFG) tensor.

In our calculations we used  $Q^{57\text{Fe}} = 0.16b$ , which was determined by Dufek, Blaha and Schwarz (1995) by comparing experimental quadrupole splitting and calculated EFG values for a large number of different Fe compounds. EFG is calculated on *ab*-

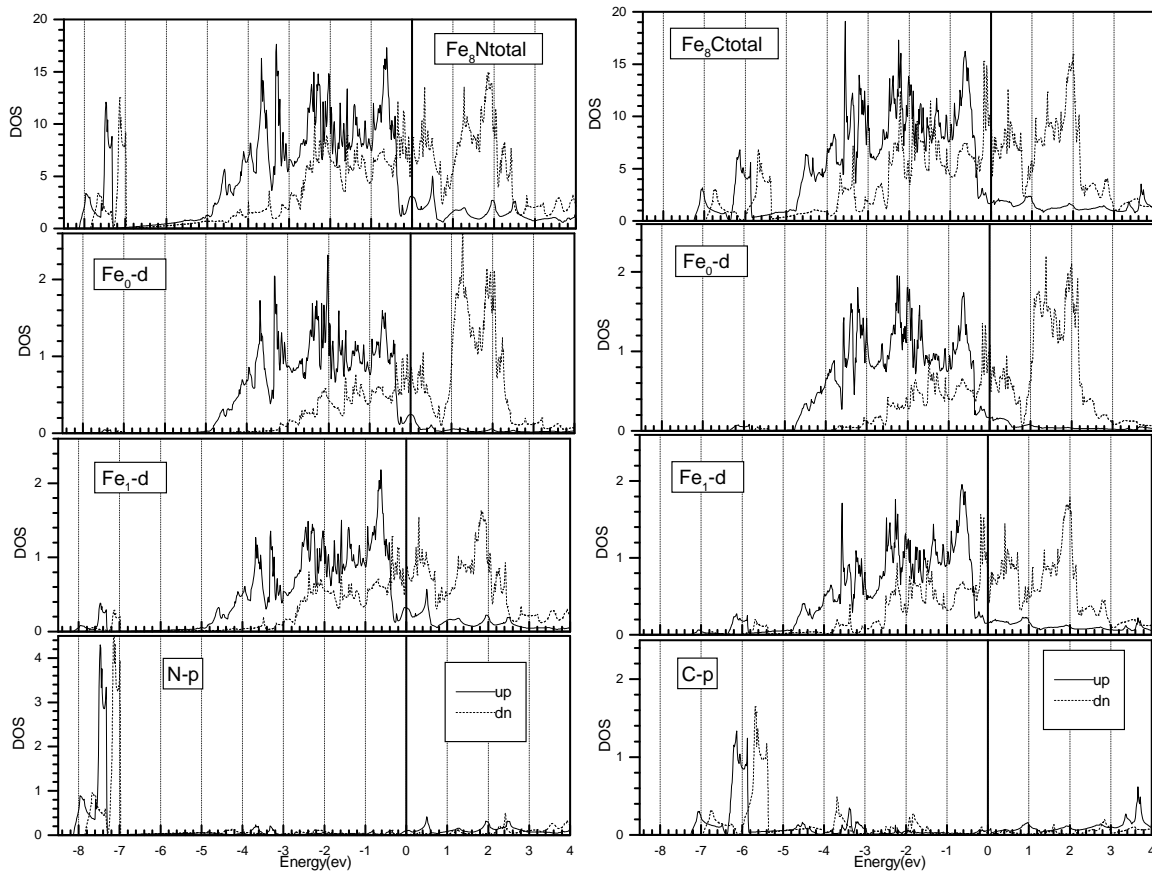


**Figure 2.** Density of states (DOS) for  $\text{Fe}_8\text{A}$  ( $\text{A}=\text{C},\text{N}$ ) compounds

*initio* basis directly from electronic density distribution using method, developed by Blaha, Schwarz and Herzig (1985).

Table 2 presents our theoretical results for quadrupole splitting as well as experimental data for carbon and nitrogen austenites, obtained by several groups. We see that reasonable agreement with experiment is obtained for Fe-C alloy. This leads to conclusion that local environment of  $\text{Fe}_1$  atom in real alloy is close to  $\text{Fe}_1$  environment in our model  $\text{Fe}_8\text{C}$  superstructure. This is also supported by the fact that according to experimental data (Bauer *et al* 1988, Gavriljuk and Nadutov 1983, Oda *et al* 1994) Fe-C austenite has only  $\text{Fe}_0$  and  $\text{Fe}_1$  atoms, which corresponds to Fe configurations in our model superstructure. On the other side, in Fe-N austenite Mössbauer spectrum is formed by contributions from  $\text{Fe}_0$ ,  $\text{Fe}_1$  and  $\text{Fe}_{2-180^\circ}$  (dumb-bell configuration) atoms (Oda *et al* 1990, Foct *et al* 1987, Gavriljuk *et al* 1990). Both absence of  $\text{Fe}_{2-180^\circ}$  atoms in our structure and bad agreement with experiment shows that Fe-N austenite can not be modeled by  $\text{Fe}_8\text{N}$  superstructure.

Our calculation shows that contribution to  $V_{zz}$  (the principal component of EFG tensor) from the regions outside the spheres (lattice EFG) is 5%, 3% and 10% for  $\text{Fe}_8\text{N}$ ,  $\text{Fe}_8\text{C}$  and  $\text{Fe}_4\text{N}$  respectively. So, for understanding of the origin of the EFG we focus on its main component, the valence EFG, which originates from the space inside the

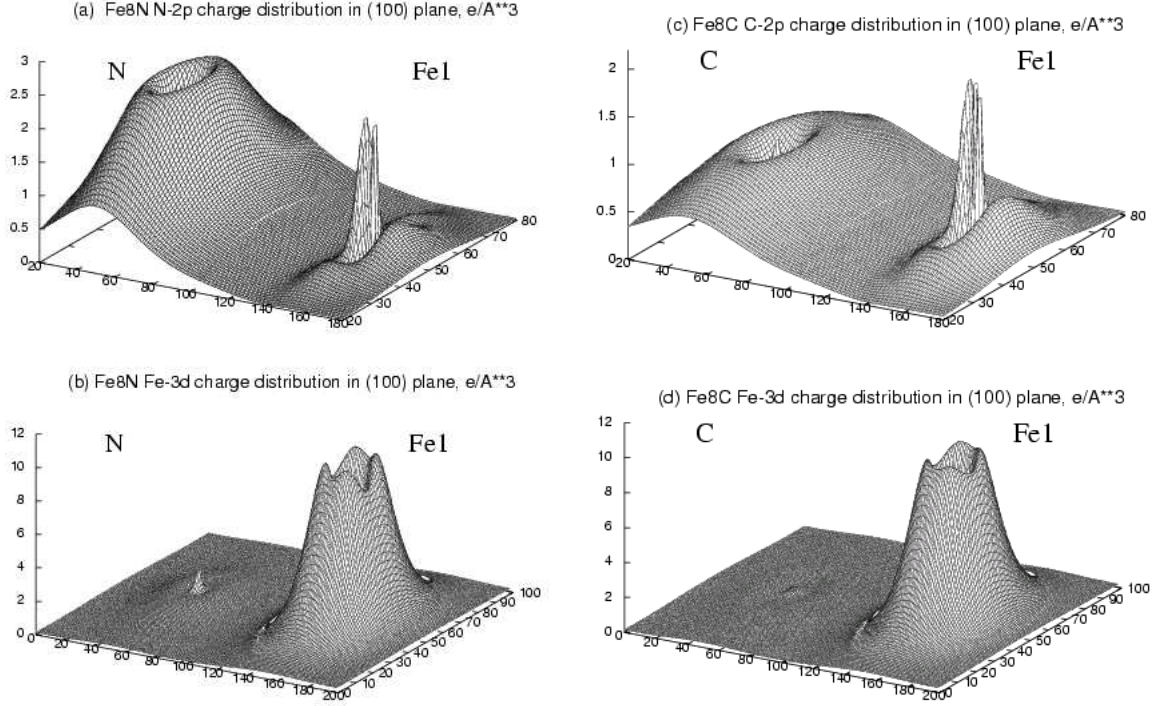


**Figure 3.** Fe<sub>8</sub>N and Fe<sub>8</sub>C charge distribution in (100) plane ( $e/\text{Å}^3$ ) for different energy regions.

atomic spheres. The ingredients for the calculation of the valence EFG are the density coefficients  $\rho_{2M}$ , which originate from two radial wave functions with  $l$  and  $l'$ :

$$\rho_{LM}(r) = \sum_{E < E_F} \sum_{l,m} \sum_{l',m'} R_{lm}(r) R_{l'm'}(r) G_{LL'}^{Mmm'}, \quad (2)$$

where  $R_{lm}(r)$  - LAPW radial wave functions,  $G_{LL'}^{Mmm'}$  - Gaunt integrals.

We performed comparative analysis of EFG formation for Fe<sub>8</sub>N and Fe<sub>8</sub>C structures. Table 2 and table 3 show that total EFG and quadrupole splitting is almost 3 times larger in Fe<sub>8</sub>C structure compare to Fe<sub>8</sub>N. By performing the analysis of mechanisms of EFG formation, we tried to find out the reasons of this considerable difference. First of all it is obvious that contribution from Fe 3s3p energy interval remains constant while going from nitrogen to carbon compound. This means that redistribution of electronic density in this region is not considerable and can not influence total EFG increasing. We observe increase of negative contribution from C 2s interval, but it is also not considerable. Moreover, the sum of contributions from impurity 2s2p energy interval remains almost constant while going from nitrogen to carbon. This means that the main reason of EFG increasing is redistribution of charge density in Fe 3d band (and partially in impurity 2p band).

In Fe<sub>8</sub>N 2p3d-band EFG contribution is positive, which decreases total EFG. In Fe<sub>8</sub>C this contribution is negative and increases total EFG. In Fe<sub>8</sub>C charge distributions in 2p and 3d bands is more symmetric than in Fe<sub>8</sub>N. While going from N to C the relative

**Table 2.** Calculated and experimental values of quadrupole splitting  $\Delta$ (mm/s) in Mössbauer spectra for Fe-N, Fe-C fcc alloys.

	Fe <sub>4</sub> N	Fe <sub>8</sub> N	Fe <sub>10.1</sub> N	Fe <sub>11</sub> N	Fe <sub>8</sub> C	Fe <sub>11.3</sub> C	Fe <sub>11.5</sub> C
$\Delta$ (theor.)	0.50	0.18			0.53		
(expt)	0.50 <sup>a</sup>		0.39 <sup>b</sup>	0.25 <sup>c</sup>		0.64 <sup>e</sup>	0.67 <sup>g</sup>
				0.39 <sup>d</sup>		0.63 <sup>f</sup>	

<sup>a</sup> Foct (1974).<sup>b</sup> Oda *et al* (1990).<sup>c</sup> Foct *et al* (1987).<sup>d</sup> Gavriljuk *et al* (1990).<sup>e</sup> Genin and Flinn (1968).<sup>f</sup> DeCristofaro and Kaplow (1977).<sup>g</sup> Oda *et al* (1994).**Table 3.** EFG analysis for Fe<sub>1</sub> atom in Fe<sub>8</sub>N and Fe<sub>8</sub>C superstructures. Contributions to valent EFG ( $10^{21}$  V/m<sup>2</sup>) from different energy bands are presented.

Fe <sub>8</sub> N	$V_{zz}^{p-p}$	$V_{zz}^{d-d}$	$V_{zz}^{val}$	Fe <sub>8</sub> C	$V_{zz}^{p-p}$	$V_{zz}^{d-d}$	$V_{zz}^{val}$
Fe3s3p	+2.448	0.000	+2.417	Fe3s3p	+2.455	0.000	+2.434
N2s	-4.369	-0.174	-4.554	C2s	-4.822	-0.354	-5.194
N2p	-4.552	-2.467	-7.067	C2p	-2.479	-3.177	-5.695
Fe3d	+0.686	+7.310	+8.074	Fe3d	-1.200	+6.309	+5.166
<i>Valent band</i>	-5.787	+4.669	-1.130	<i>Valent band</i>	-6.046	+2.778	-3.289

increasing of symmetry of  $3d$  charge distribution is much larger than relative increasing of symmetry of  $2p$  charge distribution, which leads to smaller EFG compensation and, as a result, to negative contribution from  $2p3d$ -band.

Let us now consider partial EFG contributions ( $p-p$ ,  $d-d$ ) inside Fe<sub>1</sub> sphere (other symmetry contributions like  $s-d$ , etc. are negligibly small and can not determine EFG formation). While going from N to C we observe relatively small increase of the absolute value of  $p-p$  contribution and quite large decrease of  $d-d$  contribution. As far as  $d-d$  contribution is mostly formed by own Fe $3d$  electrons, we can make a conclusion that while going from N to C the increasing of space symmetry of Fe  $3d$  electrons causes stronger influence of the asymmetric distribution of  $2s$  and  $2p$  electrons of the impurity, located in Fe<sub>1</sub> sphere.

Finally we tried to analyze the reasons of symmetry increase of  $3d$ -band charge distribution in Fe<sub>8</sub>C. Let us consider partial EFG contributions only for  $3d$ -band. In Fe<sub>8</sub>N  $p-p$  and  $d-d$  contributions are both positive and decrease total (negative) EFG. In Fe<sub>8</sub>C situation is different:  $p-p$  contribution becomes negative and its absolute value becomes twice larger. This decreases positive  $d-d$  contribution and causes the increase of total EFG.

## 5. Summary

The results of our full-potential band structure calculations of Fe<sub>8</sub>N and Fe<sub>8</sub>C structures lead to the following conclusions. We observe that in Fe<sub>8</sub>C chemical Fe-C bonding is more covalent compare to Fe-N bonding in Fe<sub>8</sub>N. Fe-C austenite can be successfully modeled by ordered Fe<sub>8</sub>C superstructure, containing iron atoms in Fe<sub>0</sub> and Fe<sub>1</sub> configurations. Calculated quadrupole splitting is in good agreement with experimental values.

We performed detailed analysis of EFG formation on Fe nuclei in this structure. The main EFG contribution is made by carbon 2s and 2p states. The contributions of these two states appear to be almost equal. Carbon states contributions are greatly canceled by asymmetry of space distribution of Fe3d-electrons.

We also calculated structure, magnetic and hyperfine interaction parameters for ordered iron nitride Fe<sub>4</sub>N structure. The results of our calculations are in excellent agreement with experimental data.

We come to conclusion that Fe-N austenite can not be modeled by Fe<sub>8</sub>N structure. The results of our calculations show that nitrogen distribution in real Fe-N alloy is different from nitrogen distribution in Fe<sub>8</sub>N structure.

## References

- Bauer Ph, Uwakweh O N C and Genin J M R 1988 *Hyperfine Interactions* **41** 555  
Bauer Ph, Uwakweh O N C and Genin J M R 1990 *Metall. Trans.* **A21** 589  
Blaha P, Schwarz K and Luitz J 1999 *WIEN97, A Full Potential Linearized Augmented Plane Wave Package for Calculating Crystal Properties* (Techn. Universitat Wien, Austria ISBN 3-9501031-0-4)  
Blaha P and Schwarz K 1983 *Int. J. Quantum Chem.* **XXIII** 1535  
Blaha P, Schwarz K and Herzig P 1985 *Phys. Rev. Lett.* **54** 1192  
Dufek P, Blaha P and Schwarz K 1995 *Phys. Rev. Lett.* **75** 3545  
Foct J, Rochegude P and Hendry A 1988 *Acta Metall.* **36** 501  
Gavriljuk V G and Nadutov V M 1983 *Fiz. Metall. Metalloved.* **55** 520  
Gavriljuk V G, Nadutov V M and Gladun O 1990 *Physics Metals Metallogr* **3** 128  
Oda K, Fujimura H and Ino H 1994 *J. Phys.: Condens. Matter* **6** 679  
Perdew J P, Burke S and Ernzerhof M 1996 *Phys. Rev. Lett.* **77** 3865  
Singh D 1994a *Plane Waves, Pseudopotentials and the LAPW method* (Kluwer Academic)  
Singh D 1994b *Phys. Rev. B* **43** 6388  
Sozinov A L, Balanyuk A G and Gavriljuk V G 1997 *Acta Mater.* **45** 225  
Sozinov A L, Balanyuk A G and Gavriljuk V G 1999 *Acta Mater.* **47** 927